

The Role of Pyrogallol as an Anti-cancer Agent Reduces Cell Proliferation in Lung Cancer Cells via AKT/PI3K Signaling Pathways - An *In vitro* and *In silico* Approaches

Prathiyangara¹, R. Priyadharshini^{2*}, Jayaraman S.³

¹Department of Pathology, Saveetha Dental College and Hospitals, Saveetha Institute of Medical and Technical Sciences (SIMATS), Saveetha University, Chennai-600 077, Tamil Nadu, India

²Department of Oral Pathology, Saveetha Dental College and Hospitals, Saveetha Institute of Medical and Technical Sciences (SIMATS), Saveetha University, Chennai-600 077, Tamil Nadu, India

³Centre of Molecular Medicine and Diagnostics (COMManD), Department of Biochemistry, Saveetha Dental College & Hospital, Saveetha Institute of Medical & Technical Sciences, Saveetha University, Chennai 600077, India

Abstract

*This study investigates the anticancer potential of Pyrogallol, focusing on its effects on cell viability, cell culture, docking analysis, and anticancer activity through fold change measurements. Pyrogallol, a naturally occurring phenolic compound, exhibits significant biological activity, including anticancer properties. This research highlights its therapeutic efficacy against specific cancer cell lines. The methodology involved culturing cancer cells under controlled conditions, followed by treatment with varying concentrations of Pyrogallol. Cell viability assays were conducted using the MTT method to evaluate cytotoxicity. Additionally, molecular docking was performed to analyze the binding interactions of Pyrogallol with target proteins implicated in cancer pathways, revealing strong affinity and specificity. Results demonstrated a dose-dependent reduction in cancer cell viability, indicating Pyrogallol's cytotoxic effects. Docking analysis revealed key interactions with critical residues in cancer-related proteins, supporting its mechanistic role in inducing apoptosis. Anticancer activity, measured by fold change in gene expression, confirmed significant upregulation of pro-apoptotic markers and downregulation of survival-associated markers. The findings underline Pyrogallol's potential as an anticancer agent with promising therapeutic implications. This comprehensive approach combining *In vitro* assays and computational analysis provides a foundation for future studies to explore Pyrogallol's clinical applications in cancer treatment.*

Keywords: Anti-cancer, Cell Proliferation, Lung Cancer, Pyrogallol, Signalling.

Introduction

Cancer remains one of the leading causes of mortality worldwide, driving an unrelenting search for innovative, effective, and less toxic therapeutic options. Among natural bioactive compounds, *Pyrogallol*, a polyphenolic substance derived from diverse natural sources, has gained increasing attention for its potent

anticancer properties [1]. This compound has demonstrated significant cytotoxicity across a wide range of malignancies, by targeting cellular pathways and mechanisms. *Pyrogallol* emerges as a promising candidate in cancer therapeutics, with studies revealing its ability to mediate cell cycle arrest, induce apoptosis, and modulate signaling cascades critical to

Received: 12.12.2024

Accepted: 27.01.2025

Published on: 31.01.2025

*Corresponding Author: priyadharshinir.sdc@saveetha.com

tumorigenesis [2]. One of the most notable applications of *Pyrogallol* lies in its activity against Hepatocellular carcinoma. Research reveals that *Pyrogallol* effectively induces S-phase arrest in Hepatocellular carcinoma cell lines such as Hep3B and Huh7 by downregulating key cell cycle regulators, including Cyclin D1, Cyclin E, and c-Myc, while enhancing the expression of tumor suppressor proteins like p27. This activity is mediated via the miR-134 axis, which plays a pivotal role in inhibiting the PI3K/AKT/Skp2/c-Myc pathway, a critical signaling cascade in cancer progression. Moreover, the inhibition of miR-134 reverses *Pyrogallol's* effects and its importance in the compound's antitumor mechanisms [3]. The utilization of nanotechnology to enhance the efficacy of *Pyrogallol* has opened new avenues in cancer treatment. For instance, *Pyrogallol* capped silver nanoparticles (py-AgNPs) synthesized using *Acacia nilotica* extract exhibit enhanced antibacterial and anticancer activities. These nanoparticles demonstrate significant cytotoxicity in Gastric adenocarcinoma (AGS) cells, induce apoptosis, and inhibit biofilm formation of *Helicobacter pylori*. Characterization studies indicate optimal particle size, stability, and biocompatibility, making py-AgNPs a promising tool for developing nanomedicine to combat gastric cancer and infections [4].

Another advancement was the encapsulation of *Pyrogallol* in nano capsules (Na-Pyr), improving its stability, bioavailability, and therapeutic efficacy. Studies have shown that Na-Pyr effectively induces apoptosis in ovarian, colorectal, and pancreatic cancer cells by modulating apoptotic pathways and enhancing oxidative stress. These findings underline the potential of nanotechnology in overcoming the limitations of conventional *Pyrogallol* delivery systems. Colon cancer is one of the most aggressive cancers, with high mortality rates. *Pyrogallol* has demonstrated significant tumor-suppressive effects in *in vivo*

models of colon cancer, reducing tumor size with minimal toxicity. By comparison, its efficacy matches standard chemotherapeutics like doxorubicin, but with reduced side effects, making it a safer alternative [5]. Similarly, in non-small cell lung carcinoma (NSCLC), *Pyrogallol* disrupts tumor progression by modulating glycolysis and the STAT2 signaling pathway. This dual-action approach impacting both metabolic and apoptotic pathways position *Pyrogallol* as a versatile anticancer agent [6].

Pyrogallol exhibits selective cytotoxicity against Neuroblastoma cells while sparing cortical neurons at lower concentrations. This specificity was attributed to its ability to reduce antioxidant enzyme levels, increasing oxidative stress selectively in cancer cells. Such properties highlight its potential as a targeted therapeutic agent, minimizing collateral damage to healthy tissues [7]. In Prostate cancer, *Pyrogallol* from *Spirogyra neglecta* inhibits proliferation and promotes apoptosis by disrupting the Akt/GSK-3 β / β -catenin signaling pathway. This activity revealed its relevance in managing cancers resistant to traditional hormonal therapies. Moreover, its ability to downregulate anti-apoptotic proteins and enhance pro-apoptotic signaling makes it a valuable asset in combating aggressive and treatment-resistant forms of cancer [8]. This study aims to analyse the role of *Pyrogallol* as an anti-cancer agent reducing cell proliferation in lung cancer cells via AKT/PI3K signaling pathways through *In vitro* and *in silico* approaches.

Materials and Methods

Plant Extract Preparation

Pyrogallol was collected from the Botanical Park in Tamil Nadu, India. The samples were washed three times with double-distilled water, then shade dried and preserved. Once dried, the samples were ground into a fine powder. Approximately 1000 g of *Pyrogallol* powder was extracted using 500 ml of ethanol over a

period of three days, with intermittent shaking to ensure thorough extraction of the constituents. The resulting extract was filtered using Whatman filter paper (Merck). This extraction process was repeated three times to achieve near complete extraction of all soluble components. The filtrates from all three extractions were then combined and concentrated by evaporating the solvents using a rotary vacuum evaporator. The final extract was stored at 4°C until further use.

Antioxidant Activity

2, 2-Diphenyl-1-picrylhydrazyl (DPPH) Free Radical Scavenging Activity

The scavenging of DPPH radicals was evaluated using the method described by Yasoth Kumar et al. (2023) [9]. Briefly, 1.0 ml of DPPH solution was added to 1.0 ml of plant extracts at various concentrations (100, 200, 300, 400, and 500 µg/ml). The mixture was then left at room temperature for 50 minutes, and the activity was measured at 517 nm. Ascorbic acid, at the same concentration range (100, 200, 300, 400, and 500 µg/ml) was used as a standard. The ability to scavenge DPPH radicals was calculated using the following formula:

$$\text{DPPH radicals scavenged (\%)} = \frac{\text{Control OD} - \text{Sample OD}}{\text{Control OD}} \times 100$$

Anti-Inflammatory Activity

Albumin Denaturation Assay

The anti-inflammatory activity of the plant extract was evaluated using the albumin denaturation inhibition method, based on the protocol, with minor modifications [10]. The reaction mixture consisted of the test extracts and a 1% aqueous solution of Bovine albumin. The pH of the mixture was adjusted using a small amount of 1N HCl. The plant extracts, at concentrations ranging from 100 to 500 µg/ml, were incubated at 37°C for 20 minutes, followed by heating at 51°C for an additional 20 minutes. After cooling, the turbidity of the samples was measured at 660 nm using a UV-

Visible Spectrophotometer (Model 371, Elico India Ltd). The experiment was conducted in triplicate, with Diclofenac used as the standard anti-inflammatory drug.

Additionally, 100 µL of Bovine serum albumin was mixed with 100 µL of *Pyrogallol* extract at varying concentrations (100-500 µg/ml) and incubated at room temperature for 5 minutes. The reaction was halted by the addition of 250 µL of trypsin, followed by centrifugation. The supernatant was collected, and absorbance was measured at 210 nm.

Calculation: % Inhibition = $\frac{\text{Absorbance of control} - \text{Absorbance of sample}}{\text{Absorbance of control}} \times 100$

Cell Culture

Human lung cancer cells (A549) were obtained from NCCS, Pune, India. The cells were regularly passaged and cultured in a CO2 incubator using a culture medium that consisted of 10% Fetal bovine serum (FBS), 1% penicillin-streptomycin antibiotic solution, and DMEM media from Himedia.

Cell Viability by MTT

This study investigated the cytocompatibility of the natural compound *Pyrogallol* against the A549 cell line using MTT and trypan blue assays [11]. A population of 1×10^4 cells was seeded and incubated overnight. After incubation, MTT reagent was added, and the resulting crystals were dissolved using DMSO. The absorbance was then measured at 590 nm.

Gene Expression by Real Time-PCR

A549 cells were seeded at a density of 5×10^6 cells per well in a 6-well plate. After overnight incubation, RNA extraction was performed using Total RNA Isolation Reagent (TRIR) from Abgene, UK. The concentration of the extracted RNA was determined through spectrophotometric quantification, measured in micrograms (µg). Subsequently, 2 µg of total RNA was reverse transcribed into cDNA following the method described by Jayaraman

et al. (2024) [12]. For mRNA expression analysis using Real-Time PCR, a reaction mixture was carefully prepared with Takara SyBr Green master mix and custom-designed forward and reverse primers targeting the PI3K/Akt gene. The thermal cycling program began with an initial activation step at 95°C for 5 minutes, followed by 30 cycles of a two-step process: denaturation at 95°C for 5 seconds, followed by combined annealing and extension for 8 seconds at the primer-specific temperature, which ranged between 56°C and 65°C. The primers were designed for the specific target gene expression analysis.

Molecular Docking Analysis

Molecular docking studies will be conducted to investigate the potential interactions between the active compounds in the *Pyrogallol* extract and target proteins. The 3D protein was gained from the Protein Data Bank (PDB). The compounds will be chosen for docking based on their high inhibitory potential. The chemical structure of the compounds will be obtained from PubChem, a chemical database.

Molecular docking simulations were performed using molecular docking software, such as PyRx, employing a grid-based approach & visualization of 2D and 3D were done by Biovia Discover studio [13].

Statistical Analysis

Data will be expressed as the Mean \pm SEM of three independent experiments, each conducted in triplicate. Statistical analysis will be carried out using one-way ANOVA, with $p < 0.05$ indicating statistical significance.

Results

The viability of lung cancer cells decreased as the concentration of *Pyrogallol* (μM) increased. A proportional reduction in cell viability was observed with rising *Pyrogallol* concentrations (Figure 1). The control revealed denser and more closely packed cells in the A549 cell line. *Pyrogallol* induced reduced cell density and altered morphology in A549 cell lines after 48 hours of treatment suggest that the treatment likely inhibited induced cell death (Figure 2).

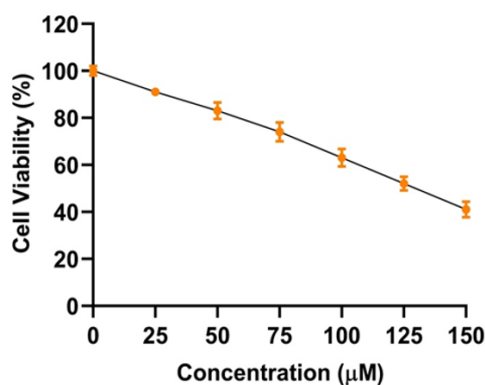


Figure 1. The Percentage of Lung Cancer Cell Viability (%) Decrease in Relation to Rise in Concentration of *Pyrogallol* (μM)

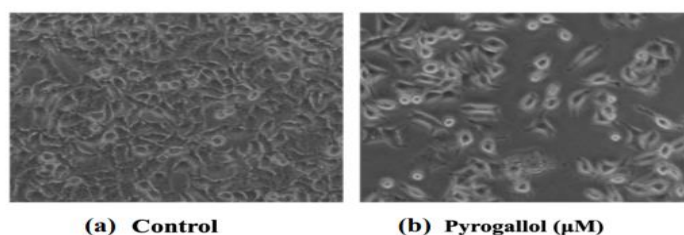


Figure 2. (a) Control Cell Line with Lung Cancer Cell Proliferation (b) A549 Cell Line Represents Decrease in Proliferation of Lung Cancer Cells with *Pyrogallol* in 48 hours.

Amplification Plot

In this graph, the x-axis represents the number of cycles in the RT-PCR process, typically ranging from 0 to 40 cycles, while the y-axis showed the Relative Fluorescence Units (RFU), which measure the fluorescence intensity emitted during PCR amplification. This intensity correlates with the amount of amplified product, with higher RFU values indicating greater gene expression. A lag phase was observed up to approximately cycle 25, where fluorescence was low, indicating minimal detectable DNA amplification. After

cycle 25–30, there is an exponential increase in fluorescence, suggesting the onset of detectable DNA amplification. The consistent and parallel rise of most curves suggests reproducibility between samples. Variability in threshold cycle (Ct) values may indicate differences in initial concentration. The Ct values for these curves appear to fall between cycles 28 and 35, depending on the specific sample. Lower Ct values indicate higher initial DNA concentrations. While the amplification of Akt/PI3K increased between cycles 30 and 40, with RFU values ranging from 400 to 480 (Figure 3).

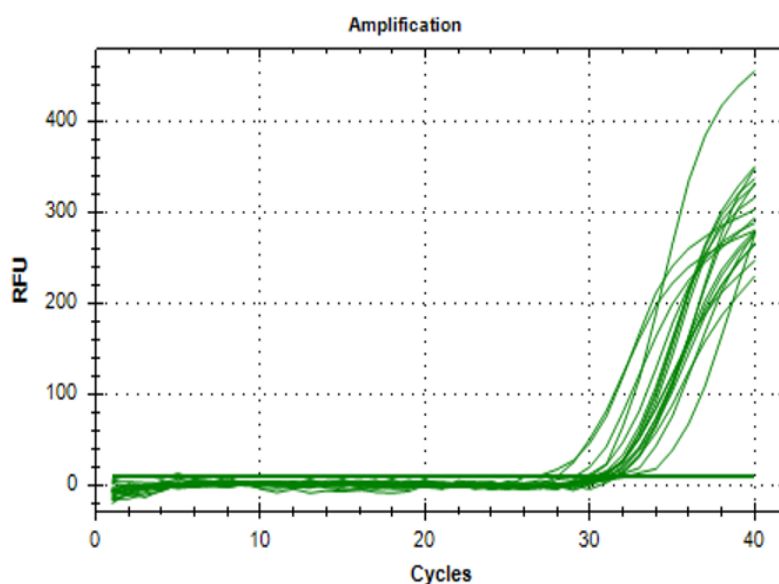


Figure 3. The Graph above Illustrates the Amplification Cycle of RT-PCR for Akt/PI3K.

Molecular Docking

Molecular docking, a valuable tool for studying a protein's active site and understanding the binding relationships between ligands and target proteins, was used to investigate the significant inhibitory effect of *Pyrogallol* on three proteins: PI3K, Akt, and RAPTOR. Notably, Akt showed the strongest impact among the extracts when compared to the standard drug reference, Ascorbic acid. The ligand appears to fit well into the binding

pocket in all panels, potentially forming strong stabilizing interactions. This is indicative of favorable binding energies that could relate to drug discovery efforts involving *Pyrogallol*, targeting specific proteins for therapeutic purposes. Comparative studies were conducted to examine the individual chemical interactions between these proteins and lung cancer cell proliferation. The results revealed that the compounds targeting Akt had the highest docking score, almost identical to the standard reference drug Diclofenac (Table 1) (Figure 4).

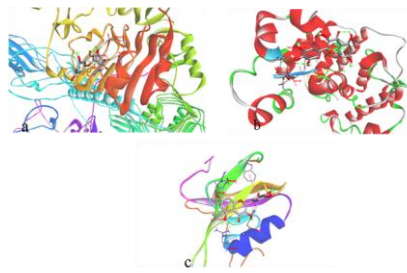


Figure 4. 3D Structure Visualized using Biovia Discovery Studio. Representation of the Docked Orientation of *Pyrogallol* and their Corresponding Counterparts Highlighting Interactions that are Critical for Biological Activity: A) PI3K, B) Akt1, and C) RAPTOR

Table 1. Molecular Docking Analysis Results using PyRx Software and 3D and 2D Structure Visualized using Biovia Discovery Studio

Compound	Targets	Binding score (Kcal/mol)
Pyrogallol	PI3K	-8.2
	Akt1	-7.1
	RAPTOR	-7.9

Gene Expression Analysis

For Akt, Mean fold change \pm S.E.M was 0.4 ± 0.05 , indicating an average 0.6-fold decrease in cancerous tissues. The results imply that the treatment decreases Akt signaling relative to β -catenin. Reduced Akt/ β -catenin levels could indicate inhibition of pathways associated with cell survival and proliferation.

PI3K expression shows a Mean fold change \pm S.E.M of 0.5 ± 0.05 , signifying a 0.5-fold decrease. RAPTOR expression presents a Mean fold change \pm S.E.M of 0.95 ± 0.01 , representing a 0.05-fold decrease on average in cancerous tissues ($p < 0.05$). Figures 5 illustrated a notable decrease in the fold change of Akt, PI3K, and RAPTOR expression in lung cancer tissue compared to healthy controls.

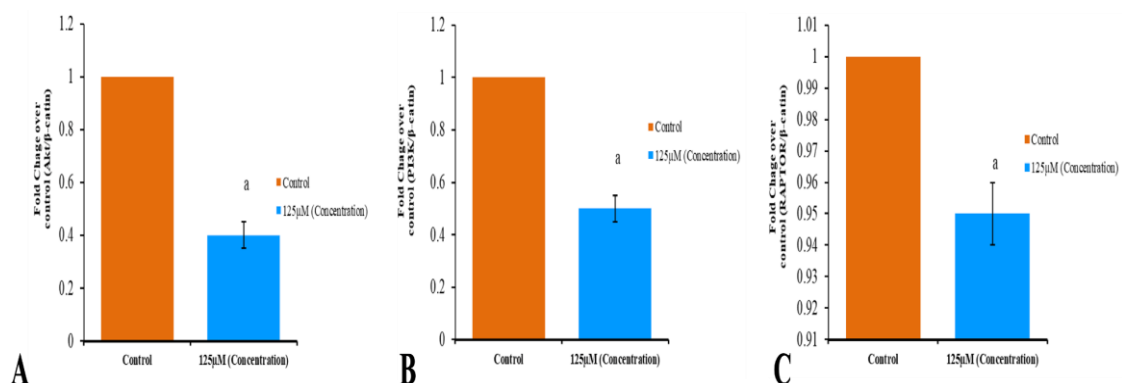


Figure 5. The bar graph represents the fold change in the expression of proteins (Akt/ β -catenin ratio) between Pyrogallol treatment at 125 μ M concentration significantly compared to the control condition, as indicated by the drop in fold change in the A549 cell line compared to healthy control. X-axis represents the fold change serving as the baseline reference. Control indicates normal A) Akt/ β -catenin B) PI3K C) RAPTOR ratio levels without treatment (Orange). At 125 μ M concentration the fold change drops significantly, indicating a marked reduction in A) Akt/ β -catenin B) PI3K C) RAPTOR ratio under treatment conditions (Blue). A label "a" over the blue bar suggests that this difference was statistically significant ($p < 0.05$).

Antioxidant Activity-DPPH Activity

The antioxidant and anti-inflammatory activity of *Pyrogallol* was evaluated using Ascorbic acid and Diclofenac. The percentage inhibition by *Pyrogallol* increased with higher concentrations, with the highest inhibition observed at 500 µg/mL. Figure 6 and Table 2 illustrates the antioxidant activity of *Pyrogallol*, demonstrating a progressive increase in inhibition percentage with rising concentrations (µg/mL). *Pyrogallol* exhibited the following Mean ± SD values for inhibition at various concentrations: 12.2 ± 1.32 (100 µg/mL), 29.43 ± 3.2 (200 µg/mL), 34.2 ± 1.45 (300 µg/mL), 52.32 ± 1.1 (400 µg/mL), and 63.43 ± 2 (500 µg/mL). These values were comparable to those of the positive control, Ascorbic acid, which showed Mean ± SD

values of 22.43 ± 2, 34 ± 0.98, 56 ± 2.1, 63 ± 1.2, and 79.54 ± 2.3 for the same concentrations (p<0.05).

The graph displays the DPPH activity (percentage of inhibition) for Ascorbic acid and *Pyrogallol*, across various concentrations (100–500 µg/mL). Both Ascorbic acid and *Pyrogallol* showed an increase in percentage of inhibition as their concentration increases, indicating a dose-dependent antioxidant activity. At lower concentrations (100–300 µg/mL), *Pyrogallol* exhibits higher DPPH activity compared to ascorbic acid. At the highest concentration (500 µg/mL), *Pyrogallol* shows significantly higher activity at 79.54% than ascorbic acid with 63.43%. *Pyrogallol* appears to be a more potent antioxidant than Ascorbic acid at higher concentrations.

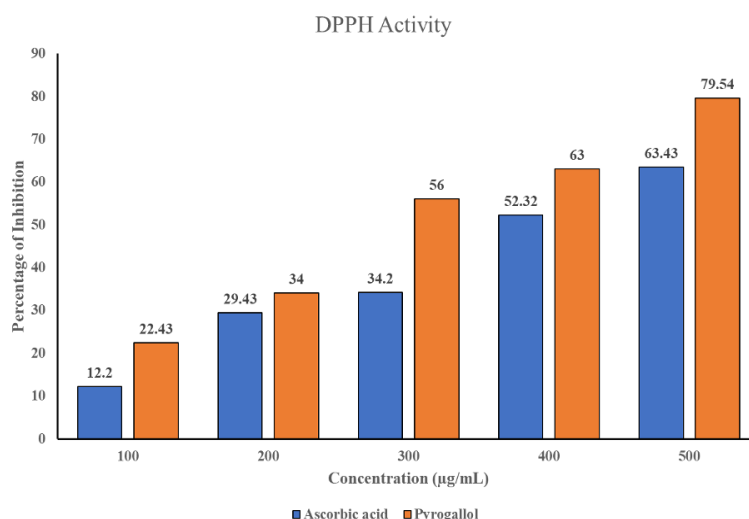


Figure 6. This Illustrates the Percentage Inhibition of DPPH by *Pyrogallol*

Table 2. The Table Displays the Mean ± SEM values for the Antioxidant activity of *Pyrogallol* Extract and a Standard at Varying Concentrations (100 µg/mL to 500 µg/mL).

Concentration (µg/ml)	Extract (Mean ± SEM)	Standard (Mean ± SEM)
100	12.2 ± 1.32	22.43 ± 2
200	29.43 ± 3.2	34 ± .98
300	34.2 ± 1.45	56 ± 2.1
400	52.32 ± 1.1	63 ± 1.2
500	63.43 ± 2	79.54 ± 2.3

Anti-inflammatory Activity

The anti-inflammatory effects of *Pyrogallol* at various concentrations were also expressed as Mean \pm SD, with higher values reflecting greater inhibition. *Pyrogallol* demonstrated inhibition values of approximately 23 ± 0.08 , 36.4 ± 0.08 , 49.65 ± 1.32 , 59.65 ± 1.78 , and

72.43 ± 3.54 ($p < 0.05$). These inhibitory effects were comparable to those of the standard drug Diclofenac. Additionally, the standard medication Metformin showed inhibition values of 38.43 ± 1.1 , 48.43 ± 0.32 , 59.98 ± 2 , 69.08 ± 1.97 , and 88.54 ± 2.93 at the same concentrations (Figure 7) (Table 3).

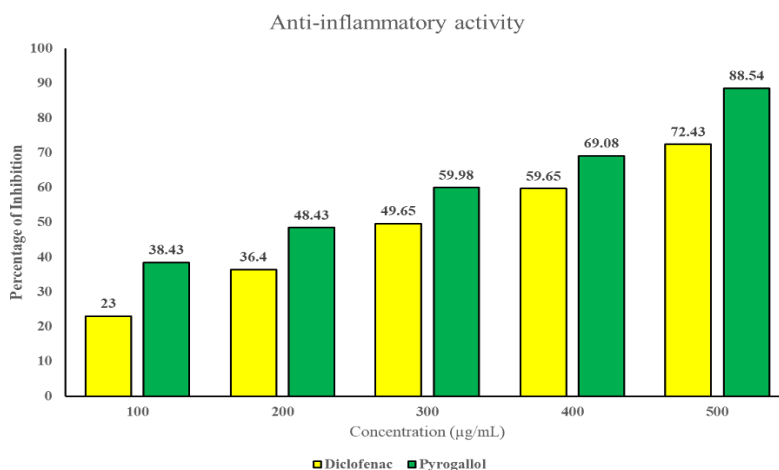


Figure 7. The graph illustrates the anti-inflammatory activity with the percentage of inhibition of two compounds, Diclofenac and *Pyrogallol*, across various concentrations (100–500 µg/mL). Both diclofenac and *Pyrogallol* show an increase in the percentage of inhibition as their concentrations rise, indicating a concentration-dependent anti-inflammatory effect. *Pyrogallol* exhibits substantially higher activity at 500 µg/mL concentration with 88.54% compared to diclofenac at 72.43%. *Pyrogallol* exhibits higher anti-inflammatory activity compared to diclofenac across all tested concentrations.

Table 3. The Mean \pm SEM values of Anti-inflammatory Activity of *Pyrogallol* Extract and Standard based on Varying Concentration

Concentration (µg/ml)	Extract (Mean \pm SEM)	Standard (Mean \pm SEM)
100	23 ± 0.08	38.43 ± 1.1
200	36.4 ± 0.92	48.43 ± 0.32
300	49.65 ± 1.32	59.98 ± 2
400	59.65 ± 1.78	69.08 ± 1.97
500	72.43 ± 3.54	88.54 ± 2.93

Discussion

Pyrogallol, a naturally occurring polyphenol, has gained attention for its significant anticancer properties. Its mechanisms of action include inducing cell cycle arrest, promoting apoptosis, and modulating critical signaling pathways such as PI3K/AKT, which are essential for cancer cell survival and proliferation. Previous studies

have demonstrated that polyphenols generally exert anti-proliferative effects on cancer cells, with *Pyrogallol* specifically showing cytotoxic and apoptogenic activity across various malignancies. These findings highlight *Pyrogallol's* potential to selectively target neoplastic cells without extensively affecting normal tissues [15,16].

Our study further supports these findings by revealing that *Pyrogallol* specifically inhibits the PI3K/AKT pathway, a major driver of tumorigenesis. This was demonstrated through molecular docking analyses, which indicated strong binding affinities for Akt (-7.1 kcal/mol) and PI3K (-8.2 kcal/mol). These interactions suggest that *Pyrogallol* can effectively disrupt the signaling cascade that promotes cancer cell proliferation and survival. Additionally, Real-Time PCR results confirmed a significant reduction in the expression levels of AKT and PI3K genes in treated A549 lung cancer cells. This downregulation reinforces *Pyrogallol's* role in targeting pathways critical to tumor progression and emphasizes its mechanism-based selectivity for cancer therapy. The therapeutic efficacy of *Pyrogallol* was further amplified by its potent antioxidant and anti-inflammatory activities. Its ability to scavenge free radicals mitigates oxidative stress, a contributing factor to cancer progression, while its anti-inflammatory effects help reduce the pro-tumorigenic microenvironment [17]. Compared to controls such as ascorbic acid (antioxidant) and diclofenac (anti-inflammatory), *Pyrogallol* demonstrated superior activity in both domains, especially at higher concentrations. These properties position *Pyrogallol* not only as an anticancer agent but also as a compound capable of modulating the cancer microenvironment, enhancing its therapeutic potential.

Previous research has highlighted the benefits of incorporating nanotechnology to overcome limitations associated with *Pyrogallol's* delivery. Formulations such as *Pyrogallol*-capped silver nanoparticles (py-AgNPs) and encapsulated nanocapsules (Na-Pyr) have been shown to improve the compound's stability, bioavailability, and tumor-targeting abilities. These advancements enhance *Pyrogallol's* efficacy and reduce systemic toxicity, paving the way for its application in clinical settings. Although nanotechnology was not explored in this study,

the promising molecular docking results suggest that integrating such techniques could further optimize *Pyrogallol's* therapeutic impact in lung cancer [18]. In vitro cytotoxicity assays on A549 lung cancer cells confirmed that *Pyrogallol* exhibits dose-dependent cytotoxic effects, significantly reducing cell viability and altering cell morphology. These findings align with earlier studies reporting *Pyrogallol's* selective cytotoxicity in various cancers. The compound's ability to induce such effects in cancer cells, while sparing normal tissue at lower concentrations, and its potential as a targeted therapeutic agent. This selectivity was particularly important in reducing the adverse effects commonly associated with conventional chemotherapy [19]. Limitations of the study include *Pyrogallol's* anticancer effects are demonstrated in vitro and through molecular docking, comprehensive in vivo studies are limited, leaving a gap in understanding its systemic effects and long-term efficacy. Studies should follow investigating the synergistic effects of *Pyrogallol* with existing chemotherapeutics may enhance its efficacy while reducing toxicity.

Conclusion

The study strongly supports *Pyrogallol's* potential as a cancer-fighting agent targeting the AKT/PI3K pathway in lung cancer cells. These results, corroborated by prior research and parallel studies on similar compounds, highlight *Pyrogallol's* promise in cancer therapy. This work paves the way for a deeper exploration of *Pyrogallol's* therapeutic potential, suggesting it could play a significant role in the development of personalized cancer treatments. Future research should focus on clinical trials and understanding the mechanisms underlying its anticancer effects.

Acknowledgement

The authors are thankful to Saveetha Institute of Medical and Technical Sciences,

Saveetha Dental College and Hospitals, and Saveetha University for providing a platform to conduct the study

Conflict of Interest

All the authors declare that there was no conflict of interest in the present study

Reference

- [1]. Gupta, A., Jeyakumar, E., Lawrence, R., 2021, Pyrogallol: a competent therapeutic agent of the future. *Biotech Env Sc*, 23(2):213-7, <https://www.envirobiotechjournals.com/AJMBES/v23i22021/AJ-15.pdf>
- [2]. Revathi, S., Hakkim, F. L., Kumar, N. R., Bakshi, H. A., Rashan, L., Al-Buloshi, M., Hasson, S. S. A. A., Krishnan, M., Javid, F., & Nagarajan, K., 2018, Induction of HT-29 Colon Cancer Cells Apoptosis by Pyrogallol with Growth Inhibiting Efficacy Against Drug-Resistant Helicobacter pylori. *Anti-cancer agents in medicinal chemistry*, 18(13), 1875–1884. <https://doi.org/10.2174/1871520618666180806104902>
- [3]. Ahn, H., Im, E., Lee, D. Y., Lee, H. J., Jung, J. H., Kim, S. H., 2019, Antitumor effect of pyrogallol via miR-134 mediated S phase arrest and inhibition of PI3K/AKT/Skp2/cMyc signaling in hepatocellular carcinoma. *International journal of molecular sciences*, 20(16):3985, <https://pubmed.ncbi.nlm.nih.gov/31426282/>
- [4]. Sampath, G., Shyu, D. J., Rameshkumar, N., Krishnan, M., Sivasankar, P., Kayalvizhi, N., 2019, Synthesis and characterization of pyrogallol capped silver nanoparticles and evaluation of their in vitro anti-bacterial, anti-cancer profile against AGS cells. *Journal of Cluster Science*, 32:549-57, <https://link.springer.com/article/10.1007/s10876-020-01813-8>
- [5]. Revathi, S., Hakkim, F. L., Ramesh Kumar, N., Bakshi, H. A., Sangilimuthu, A. Y., Tambuwala, M. M., Changez, M., Nasef, M. M., Krishnan, M., M., M., & Kayalvizhi, N., 2019, In Vivo Anti-Cancer Potential of Pyrogallol in Murine Model of Colon Cancer. *Asian Pacific journal of cancer prevention*:

Source of funding

The present project is funded by

- Saveetha Institute of Medical and Technical Sciences,
- Saveetha Dental College and Hospitals and Saveetha University
- Saveetha University

APJCP, 20(9), 2645–2651.

<https://doi.org/10.31557/APJCP.2019.20.9.2645>

[6]. Liu, H., Chang, Y., Jin, L., 2024, Pyrogallol Suppresses the Tumor Progression via Modulating Aerobic Glycolysis and STAT2 Signaling Pathway in Non-small Cell Lung Carcinoma. *Pharmacognosy Magazine*, 20(3):973-82, <https://journals.sagepub.com/doi/epub/10.1177/09731296241242542>

[7]. Cicek, B., Tgzd. A., Çiçek, B., et al. 2023, Pyrogallol Induces Selective Cytotoxicity in SH-SY5Y and Cortical Neuron Cells. *Recent Trends in Pharmacology*, 1(1):1-10, <https://dergipark.org.tr/en/pub/rtpharma/issue/77156/1260696>

[8]. Arjsri, P., Mapoung, S., Semmarath, W., Srisawad, K., Tuntiwechapikul, W., Yodkeeree, S., Dejkriengkraikul, P., 2023, Pyrogallol from *Spirogyra neglecta* Inhibits Proliferation and Promotes Apoptosis in Castration-Resistant Prostate Cancer Cells via Modulating Akt/GSK-3 β/β -catenin Signaling Pathway. *International Journal of Molecular Sciences*. 29;24(7):6452, <https://pubmed.ncbi.nlm.nih.gov/37047425/>

[9]. Yasothkumar, D., Jayaraman, S., Ramalingam, K., Ramani, P., 2023, In vitro Anti-Inflammatory and Antioxidant Activity of Seed Ethanolic Extract of *Pongamia pinnata*. *Biomed Pharmacol J*.16(4),2187-2193, <https://biomedpharmajournal.org/vol16no4/in-vitro-anti-inflammatory-and-antioxidant-activity-of-seed-ethanolic-extract-of-pongamia-pinnata/>

[10]. Praveen, G., Krishnamoorthy, K., Veeraraghavan, V. P., Jayaraman, S., 2024, Antioxidant and Anti-Inflammatory Activity of the Ethanolic Extract of *Euphorbia Hirta* Leaf Extract: An In Vitro and In Silico Study. *J Pharm Bioallied*

Sci. 16(Suppl 2): S1304-7,
<https://www.ncbi.nlm.nih.gov/pmc/articles/PMC11174252/>

[11]. Wu, H. Y., Yang, F. L., Li, L. H., Rao, Y. K., Ju, T. C., Wong, W. T., Hsieh, C. Y., Pivkin, M. V., Hua, K. F., & Wu, S. H. 2018, Ergosterol peroxide from marine fungus *Phoma* sp. induces ROS-dependent apoptosis and autophagy in human lung adenocarcinoma cells. *Scientific Reports*, 8(1), 17956. <https://doi.org/10.1038/s41598-018-36411-2>

[12]. Zuvairiya, U., Jayaraman, S., Sankaran, K., Veeraraghavan, V. P., R, G., 2024, Studies on the Effect of Piperine on Hepatocyte Nuclear Factor 1 Alpha (HNF-1 α) and Sterol Regulatory Element-Binding Protein 1c (SREBP-1c) Levels in High-Fat-Diet and Sucrose-Induced Type 2 Diabetes Mellitus Rats. *Cureus*. 16(2): e5406, <https://pubmed.ncbi.nlm.nih.gov/38481895/>

[13]. Jayaraman, S., Natararaj, S., Veeraraghavan, V. P., 2024, Hesperidin Inhibits Oral Cancer Cell Growth via Apoptosis and Inflammatory Signaling-Mediated Mechanisms: Evidence From In Vitro and In Silico Analyses. *Cureus*. 16(2): e53458, <https://pubmed.ncbi.nlm.nih.gov/38435153/>

[14]. Pazhani, J., Veeraraghavan, V. P., Jayaraman, S., 2023, Molecular docking analysis of proflavin with the Wnt pathway targets for OSCC. *Bioinformation*, 19(4):464, <https://pmc.ncbi.nlm.nih.gov/articles/PMC10563574/>

[15]. Mostafa, R. G., Abd-ElHamid, E. S., El-Bolok, A. H., Eldin, E. A., Tohamy, S. M., 2021,

Possible Effect of Pyrogallol on Tongue Squamous Cell Carcinoma SCC-25 Cells. *Minia Journal of Medical Research*, 32(2):77-87, https://mjmr.journals.ekb.eg/article_231548.html

[16]. Arjsri, P., Mapoung, S., Semmarath, W., et al. 2023, Pyrogallol from Inhibits Proliferation and Promotes Apoptosis in Castration-Resistant Prostate Cancer Cells via Modulating Akt/GSK-3/-catenin Signaling Pathway. *Int J Mol Sci*.24(7):6452, <https://pubmed.ncbi.nlm.nih.gov/37047425/>

[17]. Alavi Rafiee, S., Farhoosh, R., Sharif, A., 2018, Antioxidant activity of gallic acid as affected by an extra carboxyl group than pyrogallol in various oxidative environments. *European Journal of Lipid Science and Technology*, 120(11):1800319, <https://onlinelibrary.wiley.com/doi/abs/10.1002/ejlt.201800319>

[18]. Ghasemi, E., Bamoharram, F. F., Karimi, E., Meghdadi, P., 2024, Investigating the anticancer potential and apoptotic signaling of nanocapsule-loaded pyrogallol in ovarian cancer cells (A2780). *Results in Chemistry*, 11:101772, <https://www.sciencedirect.com/science/article/pii/S2211715624004685>

[19]. Yang, C. J., Wang, C. S., Hung, J. Y., Huang, H. W., Chia, Y. C., Wang, P. H., Weng, C. F., Huang, M. S., 2009, Pyrogallol induces G2-M arrest in human lung cancer cells and inhibits tumor growth in an animal model. *Lung cancer (Amsterdam, Netherlands)*, 66(2), 162–168. <https://doi.org/10.1016/j.lungcan.2009.01.016>